Preprints.org

Article

Not peer-reviewed version

A Conceptual Device Turning Quantum-Mechanical Interactions into Macroscopically Observable Events

J Gerhard Müller *

Posted Date: 16 May 2024

doi: 10.20944/preprints202405.1082.v1

Keywords: physical measurement; information gain; event generation; physical action; energy dissipation; spacetime extension; Landauer principle

Preprints.org is a free multidiscipline platform providing preprint service that is dedicated to making early versions of research outputs permanently available and citable. Preprints posted at Preprints.org appear in Web of Science, Crossref, Google Scholar, Scilit, Europe PMC.

Copyright: This is an open access article distributed under the Creative Commons Attribution License which permits unrestricted use, distribution, and reproduction in any medium, provided the original work is properly cited.

Preprints.org (www.preprints.org) | NOT PEER-REVIEWED | Posted: 16 May 2024 doi:10.20944/preprints202405.1082.v1

Disclaimer/Publisher's Note: The statements, opinions, and data contained in all publications are solely those of the individual author(s) and contributor(s) and not of MDPI and/or the editor(s). MDPI and/or the editor(s) disclaim responsibility for any injury to people or property resulting from any ideas, methods, instructions, or products referred to in the content.

Article

A Conceptual Device Turning Quantum-Mechanical Interactions into Macroscopically Observable Events

J Gerhard Müller

Department of Applied Sciences and Mechatronics, Munich University of Applied Sciences, D-80335 Munich, Germany; gerhard.mueller@hm.edu or jgmuegra@t-online.de

Abstract: The paper is concerned with the concept of elementary observations (EO). EOs are experimental answers to the question whether a matter-instrument interaction had taken place at the micro-scale of quantum phenomena. Focusing on the specific case of photon detection, we show that during their lifetimes EOs proceed through the four phases of initiation, detection, erasure and reset. Once generated, the observational value of EOs can be measured in units of the Planck quantum of physical action $h = 4.136 \times 10^{-15} eVs$. Once terminated, each unit of entropy of size $k_B = 8.617 \times 10^{-5}\, eV/K$, which had been created in the instrument during the observational phase, needs to be removed from the instrument to ready it for a new round of photon detection. This withdrawal of entropy takes place at an energetic cost of at least two units of the Landauer minimum energy bound of $E_{La} = \ln(2) k_B T_D$ for each unit of entropy of size k_B.

Keywords: physical measurement; information gain; event generation; physical action; energy dissipation; spacetime extension; Landauer principle

---

1. Introduction

In a recent paper we have re-considered three key experiments which had been groundbreaking in the evolution of our modern ideas of matter on the atomic, nuclear and elementary particle scales, with an informational perspective in mind [1]. The experiments re-considered were the Rutherford scattering experiments of Geiger and Marsden [2,3], the double-slit experiments with photons, electrons and other pieces of matter [4–7], and the visualization of nuclear particle trajectories in cloud-, bubble- and streaming chambers [8–10]. Considering these key experiments as questions asked to nature it was revealed that these are being answered in the form of streams of elementary observations (EO) which take the form of macroscopically observable events. These events, in the course of time, develop into spatio-temporal patterns of events, which allow conceivable alternatives of physical explanation to be distinguished.

Returning to the observation of single events, i.e., to the first step in the process of physical information gain, we came to the conclusion that the elementary observations, produced by the above key experiments, do not convey any other information other than that that an event has happened at a particular space-time location $\vec{X} = (\vec{x}, t)$. With this conclusion in mind, the process of physical information gain reveals obvious similarities to the transmission of complex messages over technical information channels [11–15]. There, meaningful messages, as for instance texts and images, emerge at the receiver end out of streams of seemingly meaningless binary digits or bits. Following this analogy, it appeared to be necessary to obtain a clearer picture of those elementary observations that had been produced in these key experiments. Final conclusion of this re-consideration process was that these elementary pieces of information feature a double nature, both as digital pieces of information, on the one hand, and as firm physical entities as pieces of physical action, on the other hand. With this first conclusion in mind, we returned to the original statement of Landauer, namely that "information is physical" [16–21].

© 2024 by the author(s). Distributed under a Creative Commons CC BY license.

Preprints.org (www.preprints.org) | NOT PEER-REVIEWED | Posted: 16 May 2024 doi:10.20944/preprints202405.1082.v1

Quantitatively we arrived at the conclusion that the pieces of physical action, $\boldsymbol{W_{obs}}$, associated with such elementary observations take the form [1]

$$\boldsymbol{W_{obs} = E_{obs}\tau_{obs} \gg h}. \quad (1)$$

where $\boldsymbol{E_{obs}}$ stands for the energy that had been spent in turning the initiating micro-events into macroscopically observable events, $\boldsymbol{\tau_{obs}}$ for the time duration during which the generated events remained observable on the macro-scale, and $\boldsymbol{h}$ for Planck's constant. While these common features could be observed in all of the above-mentioned key experiments, the discussion also revealed that experimenters, in the course of time, have invented multiple ways of turning quantum-mechanical interactions on the micro-scale into macroscopically observable events. Due to this diversity of methods and their complexity, macroscopically observable events, up to the present day, have not yet been considered as useful theoretical concepts.

In order to change this situation, we return to a key idea of Leo Szilard [22], who introduced in 1929 a cyclic process with a single-molecule gas enclosed in a simple cylinder-piston type device, to establish - with a piece of easily overseeable physics - a first quantitative connection between the concepts of abstract information and thermodynamic entropy [23–27]. Building on this general idea we develop in section 2 an event picture of a photon which visualizes a propagating photon as a stream of continuously generated and erased quanta of physical action $\boldsymbol{h}$ which are transported towards a detector, where the photon is absorbed and where a macroscopically observable detection event is triggered. In the following sections 3-8 we discuss how the tiny packages of physical action $\boldsymbol{h}$, that had been carried by the travelling photon, are being turned into macroscopically observable detection events and which values can be assigned to the ensuing EOs. Using a photo-ionization detector (PID) as a model device [28–30] we re-derive in sections 3 and 4 the above Equation 1 and show that photon detection events are hugely amplified images of the initiating photon-detector interactions that had taken place on the micro-scale. In section 5, we are concerned with the statistical significance of events, i.e., with the level of confidence that an observed event has actually been produced by an externally generated photon and not by a random thermal agitation inside the detector itself. Section 6 deals with the entropy cost of EO formation. There, it is shown that EOs with optimum values of macroscopic observability $\boldsymbol{\Omega_{EO}}$ and statistical significance $\boldsymbol{\Sigma_{EO}}$ are produced at moderate entropic cost when photon and instrument share in an evenly manner in the energy cost that needs to be expended to turn a microscopic photon-detector interaction into a macroscopically observable EO. Section 7 deals with the time evolution of EOs. There, it is shown that EO s, when looked at as functions of time, develop through the four phases of initiation, detection, erasure and reset. Section 8, finally, summarizes our results on PIDs and takes a view beyond the narrow field of photon detection.

2. Photon Propagation

Before turning to the detection process itself, we should like to consider photons, i.e., the entities to be detected as such. Photons, like any other pieces of matter, feature a dual nature either as particles or as waves. In the following we should like to show that photons, either freely propagating in particle or in wave form, can also be viewed as propagating packages of physical action with sizes equivalent to the Planck constant $\boldsymbol{h}$, and with a spacetime extension of $\boldsymbol{V_{4d}} = \left[\frac{\lambda}{2}\right]^4$ while moving through space with the velocity $\boldsymbol{c}$.

Starting point of our consideration is the Planck black-body formula [31,32] which reads

$$\boldsymbol{u(\nu, T) = \frac{8\pi(h\nu)^3}{h^2c^3}\frac{1}{\exp\left(\frac{h\nu}{k_BT}\right)-1}d\nu} \quad (2)$$

with $\boldsymbol{u(\nu, T)}$ standing for the energy density of light propagating with frequency $\boldsymbol{\nu}$ in the interior of a black body with phase speed $\boldsymbol{c}$ and $\boldsymbol{k_B}$ standing for the Boltzmann constant; $\boldsymbol{d\nu}$, finally, is a small range of frequencies centered around the frequency $\boldsymbol{\nu}$. In this equation the constant

$$\boldsymbol{K_P = \frac{8\pi(h\nu)^3}{h^2c^3}} \quad (3)$$

takes the physical dimension of

$$\boldsymbol{\dim(K_P) = \frac{eV}{cm^3Hz} = \frac{eVs}{cm^3}}. \quad (4)$$

Preprints.org (www.preprints.org) | NOT PEER-REVIEWED | Posted: 16 May 2024 doi:10.20944/preprints202405.1082.v1

While the first version is consistent with an energy density per cubic centimeter and frequency interval $\boldsymbol{dv}$, the second version has the dimensions of physical action per cubic centimeter. Putting $\boldsymbol{K_P\, V_{3d} = h}$, the 3d-volume $\boldsymbol{V_{3d}}$ associated with each package of physical action of size $\boldsymbol{h}$ emerges as:

$$\boldsymbol{V_{3d}(h)} = \frac{\mathbf{1}}{\mathbf{8\pi}}\frac{\boldsymbol{c^3}}{\boldsymbol{\nu^3}} = \frac{\mathbf{1}}{\boldsymbol{\pi}}\left(\frac{\boldsymbol{\lambda}}{\mathbf{2}}\right)^{\mathbf{3}}, \qquad (5)$$

i.e., as a volume with a side length according to half a photon wavelength $\boldsymbol{\lambda}$. With $\frac{\boldsymbol{\lambda}}{\mathbf{2}} = \frac{\boldsymbol{\pi c}}{\boldsymbol{\omega}}$ the equivalent 4-volume finally becomes

$$\boldsymbol{V_{4d}(h)} = \left(\frac{\boldsymbol{\lambda}}{\mathbf{2}}\right)^{\mathbf{3}}\left(\frac{\boldsymbol{c}}{\boldsymbol{\omega}}\right) = \left(\frac{\boldsymbol{\lambda}}{\mathbf{2}}\right)^{\mathbf{4}}. \qquad (6)$$

With a package of physical action $\boldsymbol{h}$ being associated with a definite space-time volume, a picture of a photon can be developed in which photon propagation appears as a progression of quanta of size $\boldsymbol{h}$ through space in which the transport takes place in discrete steps of length $\boldsymbol{\Delta x = \lambda/2}$ and in time steps of length $\boldsymbol{\Delta t = \tau/2}$. This picture is visualized in Figure 1. There, a sinewave is generated by the rotation of a unit vector around the origin of a circle with unit radius and with its terminal point moving along its periphery with angular speed $\boldsymbol{\omega = 2\pi/\tau}$ and an interval of arc length ranging from 0 to $\boldsymbol{2\pi}$. In this picture of wave propagation, a quantum of action of size $\boldsymbol{h}$ is generated within the first quarter of each full wave and erased again while moving through the second quarter. Upon entering the second half-wave, the package is re-generated and erased again, while arriving with zero amplitude at the onset of the second full wave period.

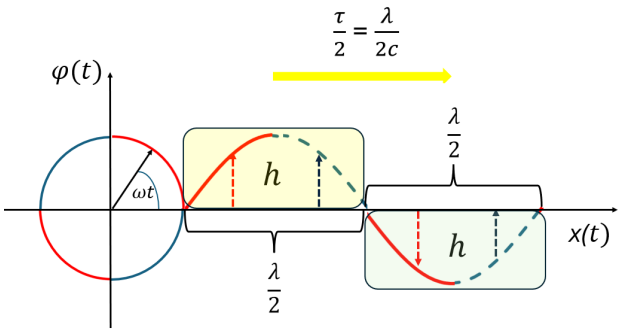

Figure 2. Propagation of an electromagnetic wave $\boldsymbol{\varphi(x,t)}$ as visualized as a shift of packages of physical action of the size of a single Planck unit h.

These considerations can be turned into mathematical form by starting from a classical electromagnetic wave of the form [30,31]

$$\boldsymbol{\varphi(x,t)} = \sin\left\{\mathbf{2\pi}\left[\frac{\boldsymbol{x}}{\boldsymbol{\lambda}} - \frac{\boldsymbol{t}}{\boldsymbol{\tau}}\right]\right\}. \qquad (7)$$

By replacing the wavelength $\boldsymbol{\lambda}$ and the frequency $\boldsymbol{\nu = 1/\tau}$ by the momentum $\boldsymbol{p_{ph}}$ and energy $\boldsymbol{E_{ph}}$ of the travelling photon, a second form of traveling wave is obtained in which a piece of action $\boldsymbol{W(x,t) = p_{ph}x - E_{ph}t}$ is generated and erased while being shifted through space.

$$\boldsymbol{\varphi(x,t)} = \sin\left\{\mathbf{2\pi}\left[\frac{\boldsymbol{p_{ph}x - E_{ph}t}}{\boldsymbol{h}}\right]\right\}. \qquad (8)$$

In essence both Figure 1 and Equation 8 more or less represent a modified version of a particle picture of wave propagation in which packages of physical action $\boldsymbol{h}$ are moved in discrete steps along a straight-line while being repeatedly generated, erased and re-generated. As this kind of transport cannot be ascertained by direct observation, we call these shifts "propagational events". Upon interaction of the photon with a piece of macroscopic matter, the propagation is stopped, and the photon energy is irreversibly dissipated. In case the photon-matter interaction occurs with a suitably designed detector, "propagational events" are intermittently transformed into "detection events" as the photon energy is being dissipated [1,30,33]. In the following we are concerned with the transformation of "propagational events" into macroscopically observable "detection events" with the help of a conceptual device.

3. Photon Detection with a Conceptual Device

Preprints.org (www.preprints.org) | NOT PEER-REVIEWED | Posted: 16 May 2024 doi:10.20944/preprints202405.1082.v1

In this section, we describe how photon-detector interactions on the micro-scale can be turned into macroscopically observable events. Discussing such interactions we aim at establishing EOs as theoretical concepts and as valid physical entities. As a model device we consider in the following photo-ionization devices (PID) in the special form of vacuum diode detectors (VDD). VDDs have found multiple applications in diverse fields of applications such as photon detection, image conversion and residual light amplification [28–30]. Key reason for choosing such devices is that these are well understood and principally able to perform as ideal photon detectors. Another key advantage is that their operational principles can be easily assessed by employing elementary physical arguments.

In order to start with, we show in Figure 2 the principle architecture of a VDD. Central component is a small cubic box with side lengths $\boldsymbol{L}$ whose walls are maintained at a temperature $\boldsymbol{T_D}$ and whose interior has been evacuated. The photons to be detected are allowed to enter the interior of the box through a small window on its top surface. On the roughened internal walls the photons are deflected, suffering multiple reflections inside the evacuated cavity until these eventually become absorbed in one of the two metal- or semiconductor electrodes which had been placed on opposite walls inside the evacuated cavity. Provided the energy $\boldsymbol{E_{ph}}$ of the trapped photon satisfies the condition $\boldsymbol{E_{ph} \geq q\phi_m}$, where $\boldsymbol{q\phi_m}$ is the work function of the metal or semiconductor electrodes, an electron can be liberated from one of the electrodes by means of the external photo-electric effect [29]. Provided a bias potential $\boldsymbol{V_b}$ is applied between both electrodes, a triangular current pulse of duration $\boldsymbol{\tau_t}$ is initiated, which flows from cathode to anode, and which can be detected with the help of the external electronic circuit, also shown in Figure 2 [28]:

$$\boldsymbol{I_s(t, L, V_b) = 2q\frac{t}{\tau_t(L,V_b)^2};\ (0 \leq t \leq \tau_t)}: \qquad (9)$$

$$\boldsymbol{\tau_t(L, V_b) = \frac{L}{c}\sqrt{\frac{2\,m_e c^2}{q\,V_b}}}. \qquad (10)$$

In this latter equation, $\boldsymbol{q}$ is the electron charge, $\boldsymbol{c}$ the speed of light, and $\boldsymbol{m_e c^2}$ the rest energy of the photoelectron.

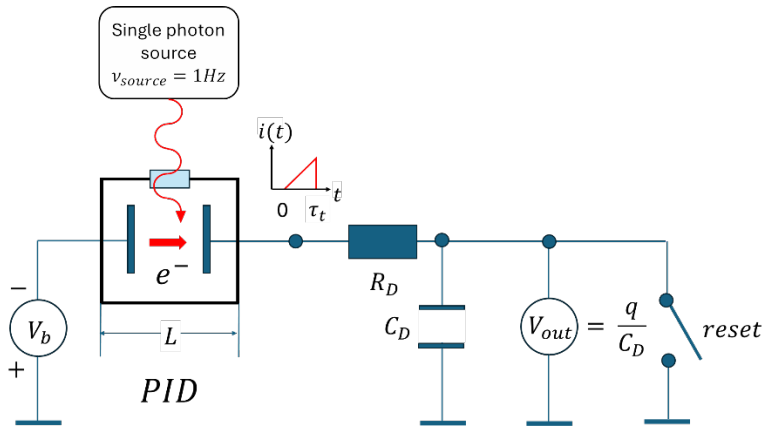

Figure 2. Schematic view onto a vacuum-diode (VDD) photon detector. While the thick read arrow inside the box indicates the internal photoelectron current flow, the thin blue lines in the exterior are electrical wires which allow for current continuity throughout the whole device; $\boldsymbol{R_D}$ and $\boldsymbol{C_D}$ form an integrator circuit which converts the very short electron pulses into quasi-permanent output voltage readings. The frequency $\boldsymbol{\nu_{source}}$ has been chosen to be much lower than the inverse transit time through the electrode gap to conform with the conditions of single-photon detection.

In considering VDDs as model devices capable of turning quantum-mechanical photon-detector interactions into macroscopically observable EOs, we neglect technical problems in device optimization and make the following principle assumptions:

- The electron work function $\boldsymbol{q\phi_m}$ can be freely chosen to vary in between the range of $\boldsymbol{0 \leq q\phi_m \leq \infty}$,

Preprints.org (www.preprints.org) | NOT PEER-REVIEWED | Posted: 16 May 2024 doi:10.20944/preprints202405.1082.v1

- The quantum efficiency $\boldsymbol{\eta}$ for turning an absorbed photon into a photoelectron is independent of photon energy and always equal to $\boldsymbol{\eta = 1}$,
- The temperature of the internal walls of the detector can be arbitrarily chosen to vary in between $\boldsymbol{0 \leq T_D \leq \infty}$,
- The device performance is not limited by any limitations inherent in the external electronics. The only limitations to device performance that will be considered are the physical limitations imposed on the variables $\boldsymbol{L}$ and $\boldsymbol{V_b}$ of the core instrument:

a) $\boldsymbol{L \geq \lambda/2}$, where $\boldsymbol{\lambda}$ is the photon wavelength, and:

b) $\boldsymbol{0 \leq V_b \leq 2m_e c^2}$.

While non-conformance to condition (a) compromises the wave-guiding properties of the evacuated cavity, non-conformance to condition (b) causes electron-positron pairs to be generated upon photoelectron impact on the anode and thus the initiation of avalanche multiplication of photoelectrons at the cathode, which terminates the parameter range of useful detector operation.

With these preparations in mind, we now develop a picture of macroscopically observable events as physical entities.

4. Making Microscopic Interaction Events Macroscopically Observable

With the functional principles of VDDs having been explained, we now turn to the problem of developing formulae for the observational value of those triangular current pulses which represent the macroscopic images of the initiating photon-detector interactions that had taken place at the cathode surface.

Multiplying Equation 10 with the bias potential $\boldsymbol{V_b}$ that had been applied across the electrode gap, the signal power

$$\boldsymbol{P_S(t, L, V_b) = 2qV_b \frac{t}{\tau_t(L,V_b)^2}} \qquad (11)$$

is obtained. Double integration of $\boldsymbol{P_S(t, L, V_b)}$ over the transit time interval $\boldsymbol{[0, \tau_t]}$, first yields the kinetic energy of the photoelectrons, which had been gained upon impact at the anode surface:

$$\boldsymbol{E_S(L, V_b) = qV_b}. \qquad (12)$$

In the second integration step the physical action is obtained which can be associated with photoelectron transits:

$$\boldsymbol{W_S(L, V_b) = \frac{1}{3} qV_b \tau_t(L, V_b)}. \qquad (13)$$

With this latter result our previously derived result of Equation 1 has been re-gained. While the electrostatic energy gain of $\boldsymbol{qV_b}$ corresponds to the energy $\boldsymbol{E_{obs}}$ that had been expended in making the photon-electron interaction on the cathode surface macroscopically observable, the electron transit time $\boldsymbol{\left(1/3\right) \tau_t(L, V_b)}$ through the electrode gap can be identified with the time $\boldsymbol{\tau_{obs}}$, during which the electron transit had remained observable.

By re-considering Equation 10 for the electron transit time $\boldsymbol{\tau_t(L, V_b)}$, it is revealed that the positive effect of making $\boldsymbol{E_{obs}}$ larger by increasing the bias potential $\boldsymbol{qV_b}$, this positive effect is partially offset by the effect of lessening time durations of the photoelectron inside the electrode gap as $\boldsymbol{qV_b}$ is increased:

$$\boldsymbol{W_S(L, V_b) = \frac{1}{3} \frac{L}{c} \sqrt{2m_e c^2 qV_b}}. \qquad (14)$$

These latter relationships are illustrated in Figures 3a,b. In considering these graphs, the most interesting fact is that the values of $\boldsymbol{W_S(L, V_b)}$ are considerably larger than the packages of physical action of size $\boldsymbol{h}$ which had been carried with the propagating photons prior to their detection. The observational values $\boldsymbol{W_S(L, V_b)}$ of the output signal currents $\boldsymbol{I_s(t, L, V_b)}$ can therefore be regarded as hugely amplified images of the microscopic interactions that had taken place at the cathode surface.

(a) (b)

Preprints.org (www.preprints.org) | NOT PEER-REVIEWED | Posted: 16 May 2024 doi:10.20944/preprints202405.1082.v1

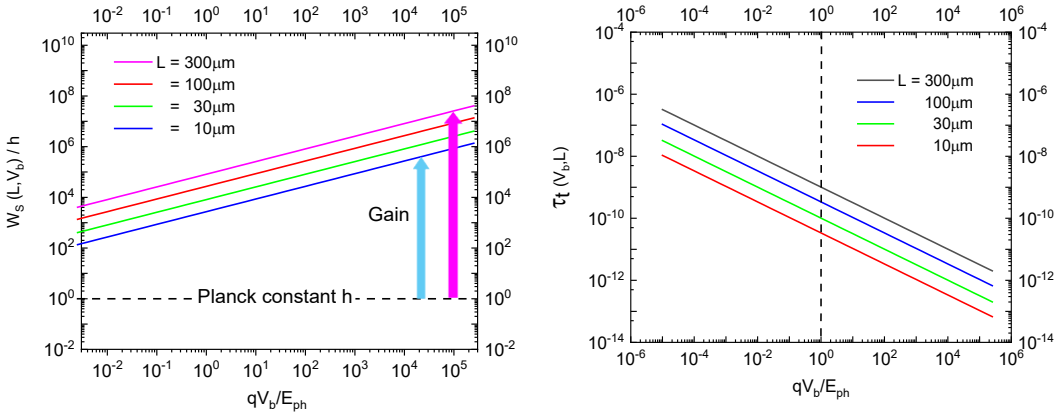

Figure 3. (a) Observational value $\boldsymbol{W_S(L,V_b)}$ as measured in multiples of the Planck constant $\boldsymbol{h}$ versus applied bias voltage $\boldsymbol{V_b}$. Parameter is the detector size $\boldsymbol{L}$; ($\boldsymbol{b}$) electron transit time through the electrode gap as a function of the applied bias voltage. Parameter: detector size $\boldsymbol{L}$.

With the relative value of $\boldsymbol{W_S(L,V_b)/h}$ representing the observational value $\boldsymbol{OV_{EO}(L,V_b)}$ of the generated EO, it is relevant to ask for limits to this possible gain. With the bias potential being raised towards its maximum value of $\boldsymbol{qV_{b\_max} = 2m_ec^2}$, the observational value emerges as

$$\boldsymbol{OV_{EO}(L,V_{b\_max}) = \frac{2}{3}\frac{m_e c\, L}{h}}, \qquad (15)$$

which shows that the observational value can principally be increased beyond any limit by making the detector size $\boldsymbol{L}$ arbitrarily large. $\boldsymbol{L}$, however, cannot be made smaller than half the photon wavelength $\boldsymbol{\lambda/2}$, because otherwise the wave-guiding condition mentioned under condition (a) above would be compromised. With visible light wavelengths varying in the range of about 700 down to 400 nm, a VDD device with side length $\boldsymbol{L \cong \lambda/2}$ would not be macroscopically observable on account of the Abbé diffraction limit [20].

5. Statistical Significance of Detected Events

Once an event had been observed, the question arises whether it had truly been generated by a photon that had originated from outside the detector and not by a random thermal agitation within the detector itself.

Figure 4 illustrates this problem of internally generated thermal noise. Shown there is a VDD without any entrance window at all. Realizing that such a device cannot detect any outside photon at all, it needs to be kept in mind that inside the detector cavity there will always be a non-zero number of thermally generated black-body photons which satisfy the detection condition of $\boldsymbol{E_{ph} \geq q\phi_m}$. Once emitted from the anode towards the cathode, such photons will generate electron transits, which fully look alike transits that had been generated by external photons.

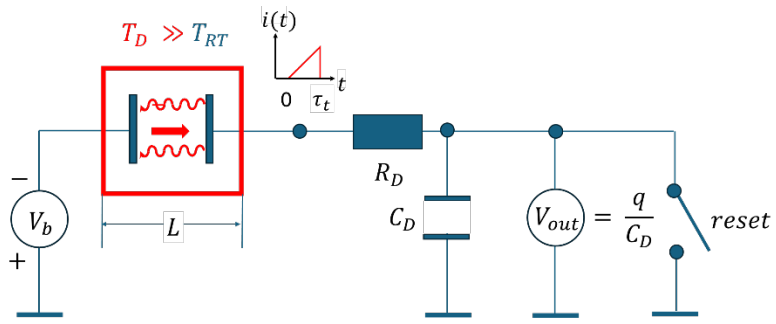

Figure 4. Blind-folded vacuum-diode detector detecting internally generated black-body radiation, i.e., random thermal noise. Sizeable amounts of black-body radiation are only generated in case the

Preprints.org (www.preprints.org) | NOT PEER-REVIEWED | Posted: 16 May 2024 doi:10.20944/preprints202405.1082.v1

detector walls are being heated to temperatures $\boldsymbol{T_D}$ much higher than room-temperature $\boldsymbol{T_{RT} \approx 300K}$.

In order to obtain a measure for the statistical significance $\boldsymbol{SI_{EO}}$ of an observed electron transit, the ratio of true versus internally generated photon needs to be evaluated. In sensorics the results of such considerations are usually expressed in terms of signal-to-noise ratios $\boldsymbol{SN}$, i.e., as ratios of the numbers of true versus noise events [28,30]:

$$\boldsymbol{SN(E_{ph}, T_D, L, V_b) = \frac{N_{true}}{N_{noise}} = \frac{1}{\sqrt{A\ \tau_t(L,V_b)\ n_{th}(E_{ph},T_D)}}}. \quad (16)$$

In this equation, $\boldsymbol{A = L^2}$ is the electrode size, $\boldsymbol{\tau_t(L, V_b)}$ the electron transit time through the electrode gap and $\boldsymbol{n_{th}(E_{ph}, T_D)}$ the areal density of photons with energies $\boldsymbol{E_{ph} \geq q\phi_m}$ that are emitted from the anode towards the cathode per unit time.

$$\boldsymbol{n_{th}(E_{ph}, T_D) = \frac{2\pi}{c^2 h^3}(k_B T_D)^3 exp\left[-\frac{E_{ph}}{k_B T_D}\right]\left\{\frac{E_{ph}}{k_B T_D}^2 + 2\frac{E_{ph}}{k_B T_D} + 2\right\}}. \quad (17)$$

Defining as the statistical significance of a detector EO the function

$$\boldsymbol{SI_{EO}(E_{ph}, T_D, L, V_b) = 1 - \frac{1}{SN(E_{ph},T_D,L,V_b)} = 1 - \sqrt{A\ \tau_t(L,V_b)\ n_{th}(E_{ph},T_D)}}\ , \quad (18)$$

a measure is obtained that assumes the value of $\boldsymbol{SI_{EO} = 1}$ when there is certainty that a detected EO had actually been generated by an outside photon, and $\boldsymbol{SI_{EO} = 0}$ when the EO is likely to have originated with equal probability either from an outside photon or from internally generated thermal noise.

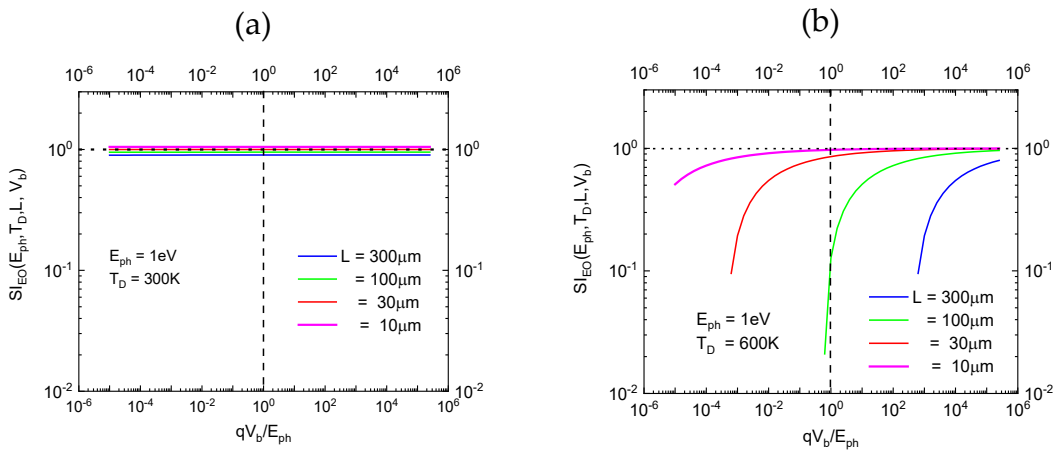

Figure 5. (a) statistical significance of EOs produced in room-temperature operated detectors. Because of low levels of internally generated black-body radiation, high-quality signals are produced at all bias levels and in all kinds of device sizes; (b) same situation as in (a), however with internal cavity walls being maintained at T = 600K.

6. Entropy Cost of Observation

The previous sections have revealed that conflicting requirements need to be met to arrive at EOs with good observational value $\boldsymbol{OV_{EO}}$ and high levels of statistical significance, $\boldsymbol{SI_{EO}}$. Whereas high values of $\boldsymbol{OV_{EO}}$ require large-size detectors, high levels of $\boldsymbol{SI_{EO}}$ require sensors with minimal sizes. In order to arrive at EOs with high overall value, compromises, obviously, need to be found. A guiding principle for finding such compromises is asking for the entropic cost that needs to be expended for attaining specific values of $\boldsymbol{OV_{EO}}$ and $\boldsymbol{SI_{EO}}$. Before we enter this discussion, let us take a brief look at entropy production and erasure of information in VDD devices.

In order to start with, consider Figures 6a,b. Both figures show in the form of semiconductor-like band profiles the fate of photoelectrons as these progress through the phases of initiation, detection, erasure and reset in the course of EO generation. While Figure 6a shows the case of an unbiassed VDD, Figure 6b shows the case of a VDD which had been biased to convert the initially

Preprints.org (www.preprints.org) | NOT PEER-REVIEWED | Posted: 16 May 2024 doi:10.20944/preprints202405.1082.v1

deposited photon energy into kinetic energy of the emitted photoelectron as it approaches the photo-anode.

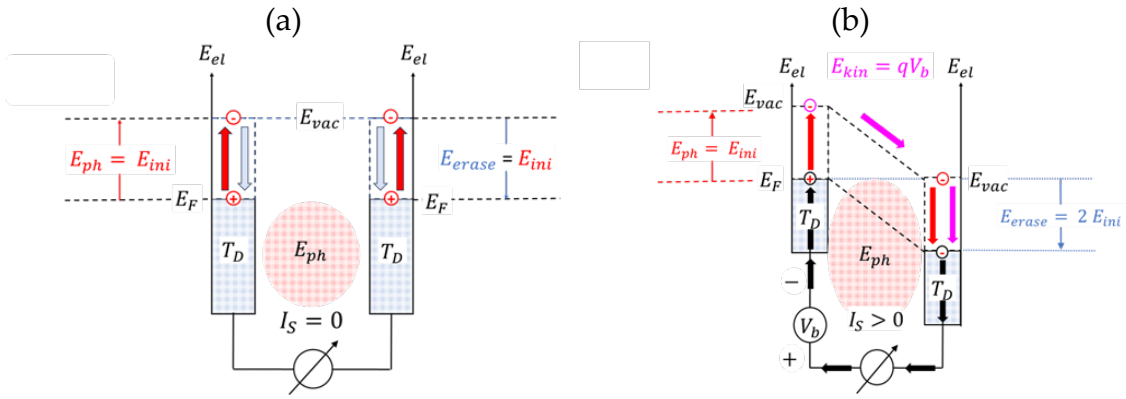

Figure 6. Pathways of photoelectrons in a band profile picture of a VDD: (a) unbiased condition; (b) bias conditions optimally chosen to convert initiating photon energy into the kinetic energy of an emitted photoelectron.

Turning to Figure 6a first, we note that in the zero-bias case photons, satisfying the minimum energy requirement of $\boldsymbol{E_{ph\_min} = q\phi_m}$, are able to produce photoelectrons at both electrodes. In such cases, electrons are removed from the Fermi energy of the affected electrode and transferred to the vacuum level at this same electrode. In this way, potential energy equivalent to $\boldsymbol{E_{pot} = E_{vac} - E_F}$ has been added to an electron while the initiating photon had been annihilated. With the energetic electron staying inside the affected electrode for a short time $\boldsymbol{\tau_{vac}}$, no displacement current is generated, and no macroscopically observable electron transient is initiated. After the time $\boldsymbol{\tau_{vac}}$ had elapsed, the excited electron returns to the Fermi level and its potential energy is broken up into $\boldsymbol{n_{th} = E_{ph}/k_BT_D}$ pieces of thermal energy of size $\boldsymbol{k_BT_D}$. With this added energy, low-temperature heat $\boldsymbol{\Delta Q = E_{ph}}$ has been added to the affected electrode and the level of ignorance, $\boldsymbol{\Delta MI_{electrode}}$, concerning its unobservable state of internal degrees of freedom, has been increased [25,30,33] by an amount of

$$\boldsymbol{\Delta MI_{electrode} = \frac{1}{ln(2)}\frac{E_{ph}}{k_BT_D}} \text{ bits.} \qquad (19)$$

After a waiting time $\boldsymbol{\tau_{diss}}$, the excess heat $\boldsymbol{\Delta Q}$, that had been generated inside the affected electrode, will have been dispersed in the wider environment of the electrode, Moreover, with each piece of energy of size $\boldsymbol{E_{La} = \ln(2)k_BT_D}$ that had diffused away from the electrode, one bit of missing information $\boldsymbol{\Delta MI_{electrode}}$, that existed before heat diffusion had taken place, had been erased.

As the information $\boldsymbol{\Delta MI_{electrode}}$ had initially been carried by the incoming photon, it can be concluded that the incoming photon had carried potential information, equivalent to

$$\boldsymbol{I_{ph}(E_{ph}, T_D) = \frac{1}{ln(2)}\frac{E_{ph}}{k_BT_D}} \text{ bits,} \qquad (20)$$

prior to detection. This amount of information simply measured its potential of creating an equivalent number of bits of $\boldsymbol{\Delta MI}$ upon absorption inside a heat reservoir of temperature $\boldsymbol{T_D}$, or in a detector operated at this same temperature. This latter issue had already been discussed in some of our previous papers [30,33].

Things change drastically when bias potentials are applied. In this case, initiation as before, involves the conversion of photon energy $\boldsymbol{E_{ph}}$ into potential energy $\boldsymbol{E_{pot} = E_{vac} - E_F}$ of a photoelectron. With the energy scale at the cathode having been upward shifted by the negative bias $\boldsymbol{qV_b = E_{ph}}$ supplied by the external voltage source (see Figure 2), the photoelectron has acquired potential energy equivalent to $\boldsymbol{E_{el} = 2E_{ph}}$ after it had been excited to the vacuum level of the photocathode. Once arrived at its surface, the electron is free to follow the externally applied electric field within the electrode gap, thus allowing it to gain kinetic energy equivalent to $\boldsymbol{E_{kin} = E_{ph}}$ upon arrival at the anode surface. Once arrived at the vacuum level of the anode, the electron still has

Preprints.org (www.preprints.org) | NOT PEER-REVIEWED | Posted: 16 May 2024 doi:10.20944/preprints202405.1082.v1

potential energy equivalent to $\boldsymbol{E_{pot} = E_{ph}}$, as the anode, unlike the cathode, had been directly connected to the ground potential of $\boldsymbol{qV_b = 0}$.

After the photoelectron had returned to the anode Fermi level, all of its acquired energy will be converted into low temperature heat

$$\boldsymbol{\Delta Q_{anode} = E_{kin} + E_{pot} = 2E_{ph}}, \quad (21)$$

thus increasing the level of uncertainty about the internal degrees of freedom inside the anode by

$$\boldsymbol{\Delta MI_{anode}} = \frac{1}{\ln(2)} \frac{E_{pot} + E_{kin}}{k_B T_D} = \frac{2E_{ph}}{E_{La}(T_D)} \text{ bits.} \quad (22)$$

As in the unbiased case, the transferred energy $\boldsymbol{\Delta Q_{anode}}$ is subsequently removed by heat diffusion and dispersed in the wider environment of the anode. With each piece of energy of size $2\,\boldsymbol{E_{La}} = \boldsymbol{2\ln(2) k_B T_D}$ leaving the anode, one bit of missing information $\boldsymbol{\Delta MI_{anode}}$ is erased and removed from the anode. With this result we have verified our earlier proposal [1] that EOs are generated at the expense of dissipating energy. What remained unanswered so far is which observational value and which level of statistical significance, as measured in units of $\boldsymbol{OV_{EO}}$ and $\boldsymbol{SI_{EO}}$, had been generated under the assumed bias condition of $\boldsymbol{qV_b = E_{ph}}$.

In order to find optimum conditions for the bias potential, we calculate the observational value of detection EOs with their values of $\boldsymbol{OV_{EO}}$ and $\boldsymbol{SI_{EO}}$ being rated against the values of $\boldsymbol{\Delta MI_{anode}}$ that had been created at the end of the detection phase inside the anode. With the definitions of section 4, we obtain for the rated observational value

$$\boldsymbol{\Omega_{EO}(E_{ph}, T_D, L, V_b)} = \frac{1}{ln(2)} ln\left\{\frac{1}{3}\left[\frac{k_B T_D}{h}\right]\left[\frac{\tau_t(L,V_b)}{(1+\frac{E_{ph}}{qV_b})}\right]\right\}, \quad (23)$$

with

$$\boldsymbol{\tau_{t\_red}(L, V_b)} = \left[\frac{\tau_t(L,V_b)}{(1+\frac{E_{ph}}{qV_b})}\right], \quad (24)$$

standing for the reduced electron transit time and $\boldsymbol{\tau_{PB}(T_D)}$ for the Planck-Boltzmann thermalization time [20,34].

$$\boldsymbol{\tau_{PB}(T_D)} = \frac{h}{k_B T_D}. \quad (25)$$

Similarly we obtain for the rated statistical significance

$$\boldsymbol{\Sigma_{EO}(E_{ph}, T_D, L, V_b)} = \frac{1}{ln(2)} ln\left\{\frac{SI_D(E_{ph},T_D,L,V_b)}{\Delta MI_{anode}(E_{ph},T_D,,V_b)}\right\}. \quad (26)$$

The values of both figures of merit (FOM) are plotted in Figures 7a,b as functions of the rated bias potential $\boldsymbol{qV_b/E_{ph}}$, showing that both FOMs do indeed take on optimum values in case $\boldsymbol{qV_b \cong E_{ph}}$. The optimum at $\boldsymbol{qV_b \cong E_{ph}}$ arises from the fact that $\boldsymbol{\Omega_{EO}}$ first increases at low bias potentials $\boldsymbol{qV_b}$ at approximately constant entropy cost as shown in Figure 3a and the inset in Figure 7a and then drops off as the entropy cost $\boldsymbol{\Delta MI}$ rapidly increases beyond $\boldsymbol{qV_b > E_{ph}}$. Turning to $\boldsymbol{\Sigma_{EO}}$, the rapidly growing entropy production at $\boldsymbol{qV_b > E_{ph}}$ overcompensates the positive effect of decreasing electron transit times in this bias potential range (see Figure 3b) and thus causes the rapid drop-off of $\boldsymbol{\Sigma_{EO}}$ beyond $\boldsymbol{qV_b = E_{ph}}$ which is displayed in Figure 7b.

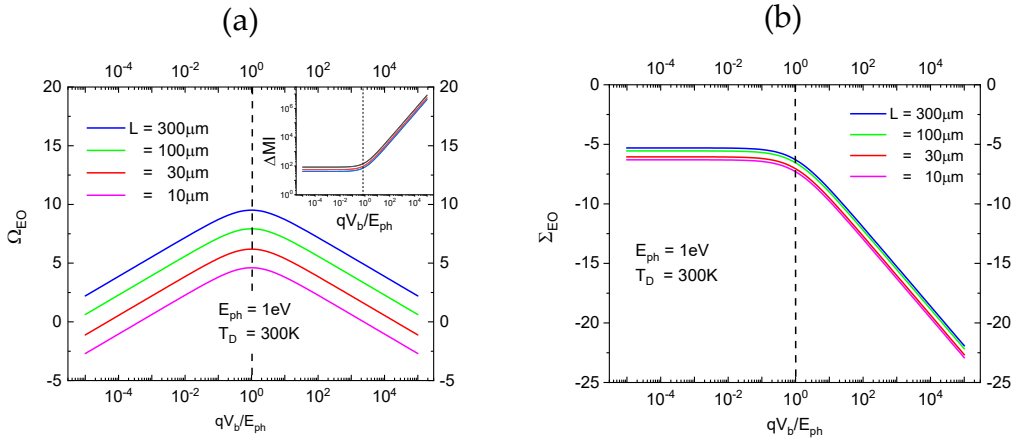

Preprints.org (www.preprints.org) | NOT PEER-REVIEWED | Posted: 16 May 2024 doi:10.20944/preprints202405.1082.v1

Figure 7. (a) Rated observability $\boldsymbol{\Omega_{EO}}$ as a function of rated bias potential $\boldsymbol{qV_b/E_{ph}}$ with the device size $\boldsymbol{L}$ as parameter. The different curves in the inset show the impact of temperate on entropy production; (b) Rated statistical significance $\boldsymbol{\Sigma_{EO}}$ as a function of the rated bias potential $\boldsymbol{qV_b/E_{ph}}$ and as evaluated for different device sizes $\boldsymbol{L}$. For clarity of presentation the curves in Figure 7b had been slightly offset from each other.

7. Time Evolution of Elementary Observations

As already mentioned above, EOs feature a transient nature, proceeding through the sequential phases of initiation, detection, erasure, and reset. Again as before, these processes are displayed in Figure 8 in the form of band diagrams.

While Figures 8a–c re-address those changes that had already been discussed in section 6 above, Figure 8d shows that, after all introduced pieces of energy had been dissipated at the anode and all ensuing bits of missing information $\boldsymbol{\Delta MI_{anode}}$ had been erased, a final step of reset is still needed to bring the instrument back to its initial state prior to photon detection. In this final step, the external voltage source needs to push the photoelectron with ground state energy $\boldsymbol{qV_b = 0}$ at the anode back up to the initial Fermi level position at the photocathode. Once again, this requires an energy $\boldsymbol{E_{reset} \cong E_{ph}}$. Once it is assumed that this shift can be affected without producing any additional entropy, the overall energetic cost for information erasure after detection remains at 2 units of $\boldsymbol{E_{La} = \ln(2)\, k_B T_D}$ per bit of erased $\boldsymbol{\Delta MI_{anode}}$ at the anode.

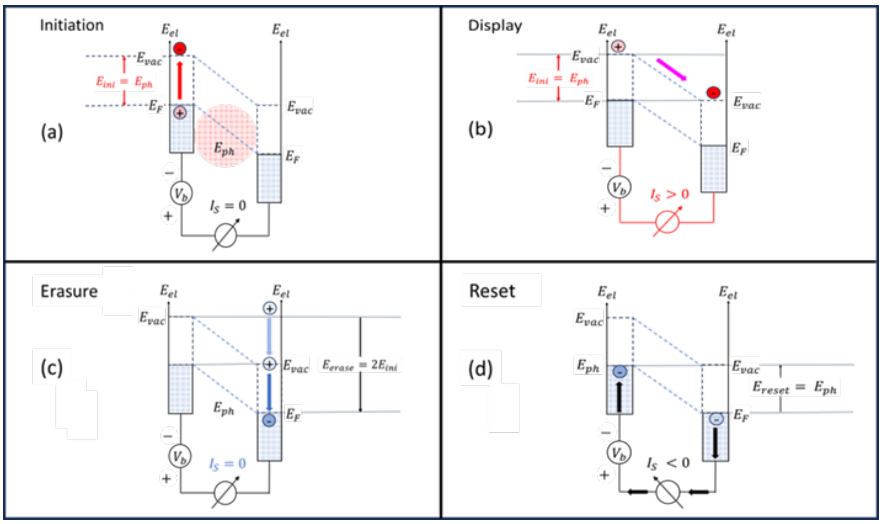

Figure 8. Band profile pictures of an EO proceeding through the sequential steps of initiation (a), display (b), erasure (c) and reset (d). After proceeding through these four steps the detector is reset in step (d) to its initial condition prior to photon absorption in step (a).

8. Summary and Conclusions

The results presented in this paper are a follow-up on our previous paper [1], in which we discussed historic experiments performed on the scale of atoms, nuclei, and elementary particles, with an informational perspective in mind. There, it has been shown that those experiments have produced complex experimental answers which are composed out of streams of elementary observations (EO) and which provide simple binary answers to the question of whether or not a matter-instrument interaction had taken place at the micro-domain of quantum phenomena.

In the present paper we have concentrated on the specific case of photon detection, and we have made use of the easily overseeable physics of vacuum-diode photon detectors (VDDD) to develop a more detailed picture of EOs, both as novel physical entities and as pieces of information. In brief, our key results are:

Preprints.org (www.preprints.org) | NOT PEER-REVIEWED | Posted: 16 May 2024 doi:10.20944/preprints202405.1082.v1

- EOs appear in the form of spatio-temporal transients with spatial dimensions larger than the observability limits set by the Abbe diffraction limit [20,34] and the temporal limits imposed by the Planck-Boltzmann equilibration time constant [20,35].
- Within the finite lifetime of EOs, EOs proceed through the four phases of initiation, detection, erasure and reset.
- EOs are pieces of physical action, formed at the expense of generating entropy and endowed with the informational properties of macroscopic observability $\boldsymbol{\Omega_{EO}}$ and statistical significance $\boldsymbol{\Sigma_{EO}}$.
- Once detected, EOs appear as macroscopic images of the initiating photon-detector interactions that had occurred at the micro-scale of quantum phenomena. The observability gain obtained in the micro-macro conversion of detection events can be measured in units of the Planck constant h. In the limit of $\boldsymbol{\Sigma_{EO} = 1}$, the generated EOs represent the binary answers concerning the initiating matter-instrument interactions that had already been discussed in our previous paper [1].
- ^ The present investigations have further shown that EOs with optimum properties of $\boldsymbol{\Omega_{EO}}$ and $\boldsymbol{\Sigma_{EO}}$ are produced when photon and detector share evenly in the energetic and entropic costs required for turning unobservable micro-events into macroscopically observable EOs. This picture of EO formation is in accordance with the view of a participatory process of information gain [36].
- Once the detection phase of EOs has ended, both the energy of the initiating photon and the energy supplied by detector-internal resources is dissipated and turned into missing information $\boldsymbol{\Delta MI_{anode}}$ concerning the unobservable microstate of the photo-anode.
- After energy dissipation had taken place, the missing information $\boldsymbol{\Delta MI_{anode}}$ is erased at an energetic cost of two units of the Landauer minimum energy bound of $\boldsymbol{E_{La} = \ln(2)\, k_B T_D}$ per bit of $\boldsymbol{\Delta MI_{anode}}$. In the final stage of reset, additional energy needs to be supplied from external resources to reset the instrument for a new round of photon detection.
- Overall, photon detection EOs appear as transiently generated and irreversibly erased one-time events in which microscopic information is transiently made available on the macro-scale.

Looking beyond the field of photon detection, we propose that the above considerations on photon detection may be generalized in diagrams as displayed in Figure 9. In this figure the cyclic process of EO initiation, detection, erasure and reset is displayed in two diagrams, with the first one emphasizing the energy inputs and outputs in the course of an EO cycle, and the second focusing on the timing issues in response to the energy inputs and outputs.

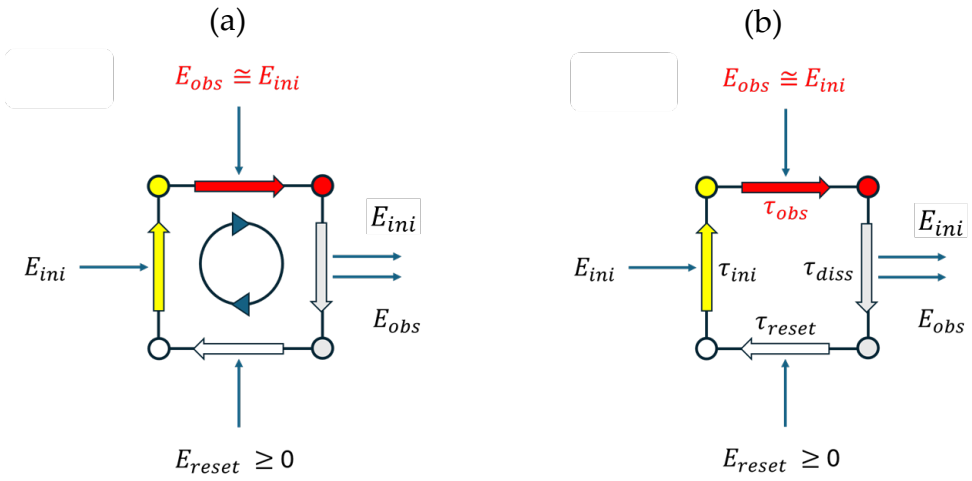

Figure 9. Generalized picture of EOs displayed as cyclic processes of initiation, detection, erasure and reset: (a) energy inputs and outputs in the different phases; (b) timing sequence of the four steps in response to energy inputs and outputs.

Preprints.org (www.preprints.org) | NOT PEER-REVIEWED | Posted: 16 May 2024 doi:10.20944/preprints202405.1082.v1

Assuming that $\boldsymbol{E_{ini} \gg k_B T}$, the parameter $\boldsymbol{\Omega_{EO}}$ is the dominant figure of merit (FOM), which characterizes the observational value of an EO. Following Equation 23 this can be approximated as

$$\boldsymbol{\Omega_{EO}(E_{ph}, T_D, L) \cong \frac{1}{ln(2)} ln\left[\frac{\tau_{obs}}{\tau_{PB}(T_D)}\right]}. \quad (27)$$

High values of $\boldsymbol{\Omega_{EO}}$ obviously rely on the efficiency of extending the observational time span $\boldsymbol{\tau_{obs}}$ of EOs beyond the Planck-Boltzmann equilibration time of $\boldsymbol{\tau_{PB}(T_D) = h/k_B T}$ which is a combination of the two natural constants of $\boldsymbol{h}$ and $\boldsymbol{k_B}$ [20,34].

Turning to the parameter $\boldsymbol{\tau_{obs}}$, the comparison in Table 1 shows that $\boldsymbol{\tau_{obs}}$ is most likely that EO-related parameter which exhibits the largest range of variability. This latter comparison shows that EOs should not be confused with the reversible thermal fluctuations of size $\boldsymbol{E_{ini} \gg k_B T_D}$ which can occur within a heat reservoir of temperature $\boldsymbol{T_D}$, and whose lifetimes $\boldsymbol{\tau_H}$ are dictated by the Heisenberg time-energy uncertainty relationship, and, which, in the case of large energies $\boldsymbol{E_{ini}}$, are much shorter than the Planck-Boltzmann thermalization time of $\boldsymbol{\tau_{PB}(T)}$ [20,34]:

$$\boldsymbol{\tau_H = \left(h/E_{ini}\right) \cong 10^{-15} s \ll \tau_{PB}(T_D) = \left(h/k_B T_D\right) \cong 10^{-13} s}. \quad (28)$$

Extremely long times of $\boldsymbol{\tau_{obs}}$, as for instance in photography, rather point to the fact that the art of creating particularly long-lived EOs relies on the art of using the energy inputs $\boldsymbol{E_{ini}}$ and $\boldsymbol{E_{obs}}$ to drive the detection instrument into a deeply trapped observational state with huge thermal release times.

Table 1. Observational lifetimes and EO figures of merit in different experimental circumstances.

EO origin	Thermal fluctuation time $\tau_{PB}(RT)$	Observational lifetime τ_{obs}	FOM_{EO}
Photon detection (PID) [this work]	$1.5 \times 10^{-13} s$	$\cong 10^{-9} s$	$\cong 12$
α- particle detection (Fluorescence) [2.3]	$1.5 \times 10^{-13} s$	$\cong 10^{-8} s$	$\cong 17$
Wilson cloud chamber [8]	$1.5 \times 10^{-13} s$	$\cong 3s$	$\cong 44$
Double-slit experiments (Photography) [4,5,6,7]	$1.5 \times 10^{-13} s$	$\cong 10^2 yr \cong 3 \times 10^9 s$	$\cong 74$

Overall, what we have achieved in the end is introducing a new vehicle of experimental information gain and information erasure which goes beyond the traditional Szilard-cylinder and piston-type approaches which had been borrowed from the age of steam engines. The proposed picture of EOs is much closer to actual experiments [1] that had been performed in unravelling processes inside the quantum domain. EOs, in addition, involve interactions of single particles with detection instruments and thus more directly conform to the requirements of minimum thermal engines.

Funding: This research received no external funding.

Institutional Review Board Statement: Not applicable

Conflicts of Interest: The author does not declare any conflict of interest

References

1. Müller, J. G. Events as elements of physical observation: Experimental evidence. Entropy 2024, 26(3),255; https://doi.org/10.3390/e26030255
2. Geiger H.,Marsden E. On a Diffuse Reflection of the α-Particles. Proceedings of the Royal Society, Series A 1909, 82, 495–500.

Preprints.org (www.preprints.org) | NOT PEER-REVIEWED | Posted: 16 May 2024 doi:10.20944/preprints202405.1082.v1

3. Rutherford, E. The Scattering of α and β Particles by Matter and the Structure of the Atom, Phil. Mag., Series 6, 1911, 21, p. 669-688.
4. Meschede. D.: Youngs Interferenzexperiment mit Licht. In Die Top Ten der schönsten physikalischen Experimente Fäßler, Fäßler, A., Jönsson, C. (Eds.). Rowohlt Verlag, Hamburg, Germany, 2005, ISBN 3-499-61628-9, pp 94–105.
5. Jönsson, C.: Electron Diffraction at Multiple Slits. American Journal of Physics 1974, 42, 4–11.
6. Carnal, O., Mlynek, J. Young's double-slit experiment with atoms: A simple atom interferometer. Phys. Rev. Lett. 1991, 66, 2689–2692, doi:10.1103/PhysRevLett.66.2689.
7. Nairz, O., Arndt, M, Zeilinger, A: Quantum interference experiments with large molecules. American Journal of Physics. 2003, 71(4), 319–325, doi:10.1119/1.1531580
8. Wilson, C. T. R. On a Method of Making Visible the Paths of Ionising Particles through a Gas. Proceedings of the Royal Society of London A: Mathematical, Physical and Engineering Sciences. 1911, 85, 578.
9. Glaser, D. A. Some Effects of Ionizing Radiation on the Formation of Bubbles in Liquids. Phys. Rev. 1952, 87(4), 665. doi:10.1103/PhysRev.87.665 (english).
10. Griffiths, L, Symoms, Ch., R. Zacharov, B. Determination of particle momenta in spark chamber and counter experiments. CERN Yellow Reports: Monographs. CERN-66-17
11. Shannon, C.E. *A Mathematical Theory of Communication*. Bell Syst. Tech. J. **1948**, 27, 379–423 & 623–656.
12. Young, J., F. *Einführung in die Informationstheorie*, R. Oldenbourg München, Wien **1975**.
13. Kraus, G. *Einführung in die Datenübertragung*; R. Oldenbourg Verlag, München, Wien, **1978**.
14. LeSurf, J., C., G. Information and Measurement. I. O .P. Publsihing Ltd. Bristol and Philadelphia, ISBN 0 7503 0308 5. **1995**.
15. Ben-Naim, A. Information Theory; World Scientific: Singapore, **2017**.
16. Landauer, R. *Irreversibility and heat generation in the computing process*. IBM J. Res. **1961**, 5, 183–191.
17. Landauer, R. *Information is physical*. Phys. Today **1991**, 44, 23–29.
18. Landauer, R. *Minimal energy requirements in communication*. Science **1996**, 272, 1914–1918.
19. Bormashenko, E. *The Landauer Principle: Re-Formulation of the Second Thermodynamics Law or a Step to Great Unification?* Entropy **2019**, 21(10), 918; https://doi.org/10.3390/e21100918.
20. Bormashenko, E. submitted to Entropy **2024**, doi: 10.20944/preprints202404.0430.v1
21. Witkowski, C., Brown, S., Truong, K. On the Precise Link between Energy and Information. Entropy 2024, 26(3), 203; https://doi.org/10.3390/e26030203
22. Szilard, L. Über die Entropieverminderung in einem thermodynamischen System bei Eingriffen intelligenter Wesen. Z. Phys. 1929, 53, 840–856. (In German)
23. Leff, H.S.; Rex, A.F. Maxwell's Demon: Entropy, Information, Computing; Adam Hilger: Bristol, UK, 1990
24. Leff, H.S.; Rex, A.F. Maxwell's Demon 2: Entropy, Classical and Quantum Information, Computing, 1st ed.; Adam Hilger: Bristol, UK, 2003; ISBN 10:0750307595; 13:9780585492377.
25. Ben-Naim, A. A Farewell to Entropy: Statistical Thermodynamics Based on Information; World Scientific: Singapore, 2008. [Google Scholar]
26. Ben Naim, A. Shannon's Measure of information and Boltzmann's H-Theorem. Entropy 2017, 19, 48.
27. Ben Naim, A. An Informational Theoretical Approach to the Entropy of Liquids and Solutions. Entropy 2018, 20, 514.
28. Kingston, R.H. Detection of Optical and Infrared Radiation; Springer: Berlin/Heidelberg, Germany, 1978. [Google Scholar
29. https://en.wikipedia.org/wiki/Photoelectric effect
30. Müller, J.G. Photon detection as a process of information gain. Entropy 2020, 22, 392.
31. Schpolski, E.W. *Atomphysik.* VEB Deutscher Verlag der Wissenschaften: Berlin, Germany, **1970**.
32. Nolting, W. Grundkurs Theoretische Physik 5/1.Springer, Berlin, Heidelberg, ISBN 978-3-540-68868-6, doi: 10.1007/978-354068869-3, **2001**.
33. Müller, J.G. Information contained in molecular motion, Entropy 2019, 21(11), 1052; https://doi.org/10.3390/e21111052
34. Liu, Y.C.; Huang, K.; Xiao, Y.-F.; Yang, L.; Qiu, C.W. What limits limits?. Nat. SCI.Rev., 2021, 8(1), nwaa210.
35. Proesmans. K.; Erich, J.; Bechhoefer, J. Optimal finite time bit erasure und der full control, Phys. Rev. E2020, 102,032105
36. Wheeler, J. A. *Information, physics, quantum: The search for links*. Proceedings of the 3rd International Symposium

Disclaimer/Publisher's Note: The statements, opinions and data contained in all publications are solely those of the individual author(s) and contributor(s) and not of MDPI and/or the editor(s). MDPI and/or the editor(s) disclaim responsibility for any injury to people or property resulting from any ideas, methods, instructions or products referred to in the content.